Journal of ELECTRONIC MATERIALS, Vol. 48, No. 10, 2019
https://doi.org/10.1007/s11664-019-07503-0
© 2019 The Minerals, Metals & Materials Society

Electrical Bistable Properties of P-25 TiO_2 Nanoparticles Composited with PVP for Memory Devices

P. UKAKIMAPARN,[1] D. CHANTARAWONG,[1] P. SONGKEAW,[1] K. ONLAOR,[1,2,3] T. THIWAWONG,[1,2] and B. TUNHOO[1,2]

1.—Electronics and Control System for Nanodevice Research Laboratory, College of Nanotechnology, King Mongkut's Institute of Technology Ladkrabang, Chalongkrung Road, Bangkok 10520, Thailand. 2.—Thailand Center of Excellence in Physics, Commission on Higher Education, Ministry of Education, 328 Si Ayutthaya Road, Bangkok 10400, Thailand. 3.—e-mail: korakot.onlaor@gmail.com

In this work, P-25 titanium dioxide nanoparticles (TiO_2 NPs) were composited with poly-vinylpyrrolidone (PVP) at various concentrations of TiO_2 NPs. The bistable memory devices were fabricated by spin coating from a prepared PVP:TiO_2 NPs solution on indium tin oxide (ITO) electrodes with the device structure of ITO/PVP:TiO_2 NPs/Al. The maximum ON/OFF current ratio of the bistable memory devices was approximately 10^5 at a reading voltage of +1 V. The mechanism of the memory device can be expressed by theoretical fitting between the experimental results and conduction models. Moreover, a retention time test for continuous read operations of the device is presented.

Key words: Titanium dioxide, nanoparticles, bistable device, memory

INTRODUCTION

Nanocomposite materials such as ceramic matrix nanocomposites and metal matrix nanocomposites have recently attracted extensive research interest due to many outstanding properties.[1] Metal oxides embedded in host polymers play roles in many applications including reinforcement material and biocompatible materials.[2,3] Moreover, metal oxide/polymer nanocomposites can be used for various electronic applications as biomedical devices, optoelectronic devices, sensors and memory devices.[4] Recently, several papers have been published concerning resistive switching and bistable memory devices.[5–7] Bistable memory devices offer benefits including simple structure, simple processes and low operation voltage.[8,9] One bistable memory structure receiving significant study consideration comprises nanoparticle blending in polymer materials.[10–12]

Titanium dioxide nanoparticles (TiO_2 NPs) fall into the metal oxide material group and have attracted attention for study and research in many fields. TiO_2 NPs exhibit more advantageous properties for various fields of applications, such as photocatalysis, solar cells, sensors and other applications.[13] Particularly, TiO_2 NPs have been studied in the area of bistable memory devices.[14,15] Among polymer materials, polyvinylpyrrolidone (PVP) polymer has been studied extensively in the field of electronic device applications due to its good stability under room temperature, low operation voltage, easy preparation and acceptable electrical properties.[16,17]

In this work, a composite film of PVP polymer and P-25 TiO_2 NPs (PVP:TiO_2 NPs) was used as an active layer of a bistable memory device with the final structure of ITO/PVP:TiO_2 NPs/Al. The conduction mechanisms of the bistable memory device are proposed to explain the switching current state from OFF state to ON state, as described in the current–voltage (I-V) results.

EXPERIMENTAL

PVP and P-25 TiO_2 NPs were purchased from Sigma-Aldrich Company. The properties of TiO_2 NPs had been investigated by x-ray photoelectron

(Received March 22, 2019; accepted July 30, 2019; published online August 8, 2019)

spectroscopy (XPS) and x-ray diffraction (XRD; see supplementary Figure S1 and S2). To fabricate the memory device, the PVP was dissolved in ethanol at a concentration of 50 mg/ml. Subsequently, P-25 TiO_2 NPs were mixed together with the PVP solution at concentrations of 2 wt.%, 4 wt.%, 6 wt.%, 8 wt.% and 15 wt.%. Then, the PVP:TiO_2 NPs solution was spin-coated on the ITO/glass substrate at a speed of 1500 rpm for 15 s. Finally, an aluminum (Al) top electrode was deposited on the PVP:TiO_2 NPs film using the thermal evaporation technique. A schematic of the bistable memory device is shown in Fig. 1. The electrical properties of the device were identified by I-V measurement. A current source meter (Keithley 2410) with computer control programming was used to acquire the I-V characteristics. The conduction mechanisms of the bistable device were fitted with a theoretical model.

RESULTS AND DISCUSSION

Figure 2 shows plan-view, bright-field, transmission electron microscopy (TEM) images of the PVP:TiO_2 NPs composite at various concentrations of TiO_2 NPs at 2%, 8% and 15%, respectively. It was found that the amount of TiO_2 NPs is seen to increase with increasing TiO_2 NPs concentration. The TiO_2 NPs are rather uniformly distributed in the PVP at sizes of approximately 20–30 nm.

Figure 3 exhibits the I-V characteristics of the ITO/PVP:TiO_2 NPs/Al bistable memory devices under a compliance current of 3 mA. Voltages were swept in the direction curve 1 to 4 with the different concentrations of TiO_2 NPs. In the case of the PVP layer only, a small hysteresis is observed, as shown in Fig. 3a, which might have resulted from the effects at the polymer and metal interface.[18–20]

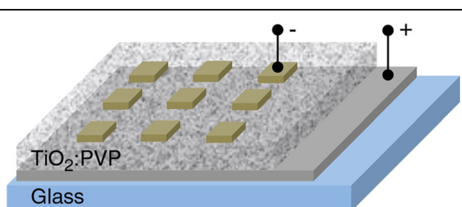

Fig. 1. The structure of the ITO(+)/PVP:TiO_2 NPs/Al(–) bistable memory device.

However, when the TiO_2 NPs concentration was increased, the TiO_2 NPs in the films show the effects on the memory property, especially the ON/OFF current ratio (other TiO_2 NPs concentrations, see supplementary Figure S3). The ON state and OFF state current correspond to a high-current state and a low-current state in a typical memory device, respectively. At the first sweep (curve 1) in Fig. 3b–d, the device has a low-conductivity state before switching to a high-conductivity state (curve 2). The different high-conductivity states between curves 1 and 2 represent the ON/OFF current ratio of the ITO/PVP:TiO_2 NPs/Al bistable memory device. After the voltages were swept back (curves 3 and 4) the conductivity states of the device were left in the ON state without transition to the OFF state again, and there was an indication of nonvolatile write-once-read-many-times (WORM) memory behavior.[8,10,21,22] The ON/OFF current ratio (read at +1 V) of each concentration exhibited the highest ON/OFF current ratio with TiO_2 NPs of 8 wt.%. Therefore, the ITO/PVP:TiO_2 NPs (8wt.%)/Al (Fig. 3c) was used for further study in the next section. However, some studies have reported that memory devices can be switched back to the OFF state after enough opposite writing voltage is applied.[23,24] Nevertheless, the reset process in this work was not observed from the applied voltage range of 7 V to -7 V. As a comparison to other polymer/NP composited studies, G. Liu et al.[25] reported that WORM memory devices were based on poly(N-vinylcarbazole), or PVK, composited with a carbon nanotube (CNT). The electrons were trapped at the CNT and permanently blocked by the PVK blocking layer. In addition, WORM memory devices based on metal oxide (ZnO NPs) embedded in polymethylmethacrylate (PMMA) were reported by T. T. Dao et al.[26] The charge-trapping process was used to explain the conduction mechanisms. For the ITO/PVP:TiO_2 NPs/Al memory structure, the PVP covering TiO_2 NPs in the layer could act as a blocking layer due to the wide energy gap of the PVP material.[27] While the TiO_2 NPs act as a trapping center inside the layer, most electrons are trapped and cannot be released. Hence, the devices show WORM memory behavior.

To understand the conduction mechanisms in the memory device prepared with a TiO_2 NPs concentration of 8 wt.%, the I-V data were used to fit by

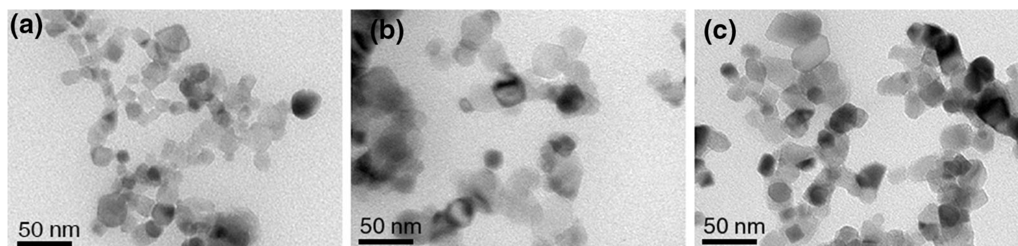

Fig. 2. TEM images of PVP:TiO_2 NPs at various concentrations of TiO_2 NPs: (a) 2 wt.%, (b) 8 wt.% and (c) 15 wt.%.

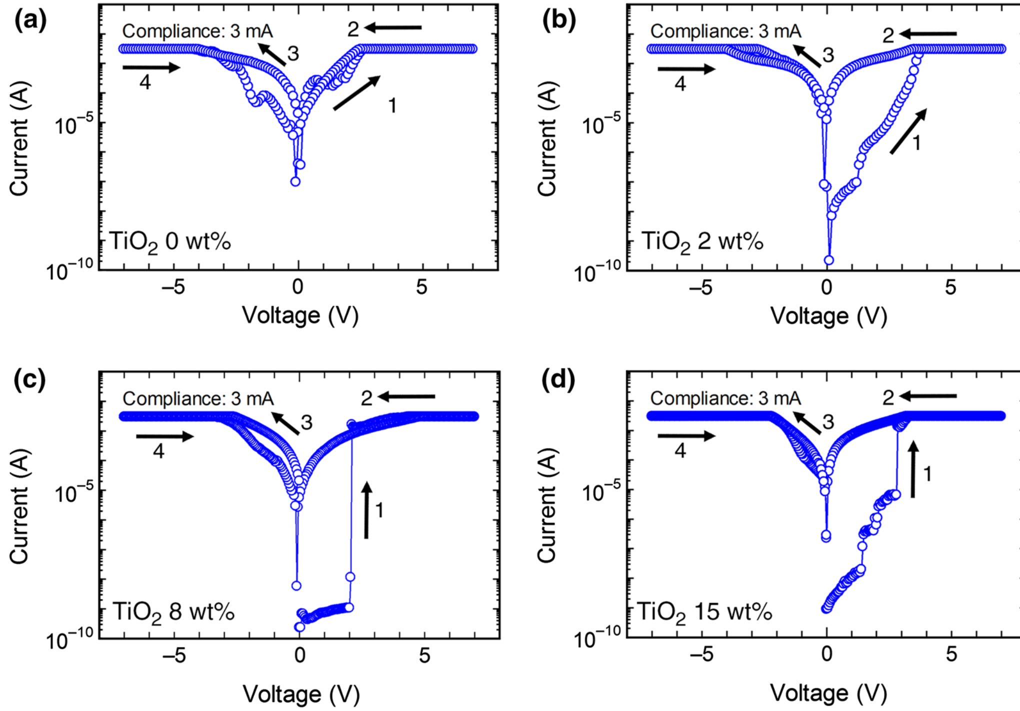

Fig. 3. I-V characteristics of the ITO/PVP:TiO_2 NPs/Al bistable memory devices with different TiO_2 NPs concentrations: (a) 0 wt.%, (b) 2 wt.%, (c) 8 wt.% and (d) 15 wt.%.

using I-V models to explain the electron transport of the device. The ln|I| versus $V^{1/2}$ plot of the OFF state can be explained as the thermionic emission process, as shown in Fig. 4a, expressed as[28,29]:

$$I = T^2 \exp\left[\frac{-(\phi_b - q\sqrt{qV/4\pi\varepsilon_i d})}{k_b T}\right], \quad (1)$$

where T is the measured temperature, ϕ_b is the barrier height at the interface, ε_i is the dynamic permittivity of the film, q is the electron charge, k_b is the Boltzmann constant and d is the film thickness. In the OFF state, the injected electrons were able to overcome the barrier height at the interface by thermal injection.[28,29] Therefore, the electrons were trapped by the trapping states until the trapping states were filled. As a result, the memory device switched to the ON state. After that the device changed from the OFF state to the ON state, a log(I) versus log(V) plot in the ON state was observed, as shown in Fig. 4b. A linear relationship with a slope of 1.311 was observed. Therefore, the conduction mechanism of the ON state is believed to exhibit an ohmic behavior, expressed as[29–31]:

$$J = \sigma E = q\mu n \frac{V}{d}, \quad (2)$$

$$n = N_C \exp\left[\frac{-(E_C - E_F)}{k_b T}\right] \quad (3)$$

where σ is the electrical conductivity, E is the electrical field, n is the number of electrons, $E_C - E_F$ is the activation energy and N_C is the effective density of states. When the voltages were applied to negative voltages, the conduction mechanism of the ON state could be also explained by ohmic conduction because the I-V behavior was similar to the ON state in the positive voltage region. The results confirmed that the captured electrons were permanently trapped at the TiO_2 NPs. Hence, the memory device could not recover the OFF state after the writing process.

To propose the conduction mechanisms of the fabricated memory device, energy band diagrams are shown in Fig. 5. It is well known that P-25 TiO_2 NPs contain anatase and rutile phases at a ratio of about 3:1.[32] The energy bandgap of anatase and rutile phases have been accepted and reported to be 3.2 eV and 3.0 eV, respectively.[33] At the initial state (Fig. 5a), the electrons were injected from the Al electrode into the PVP:TiO_2 NPs layer by thermal injection that corresponds to the thermionic emission conduction process. After that, the injected electrons were captured inside the layer at the trap state. In these processes, the device exhibited the OFF state current. When the electrons are filled into the TiO_2 NPs trapping state, the injection of electrons is free from the trapping states. Thus, the conductivity state of the device changes to the ON state, as shown in Fig. 5b. For the reverse direction, the trapped electrons could not be released because

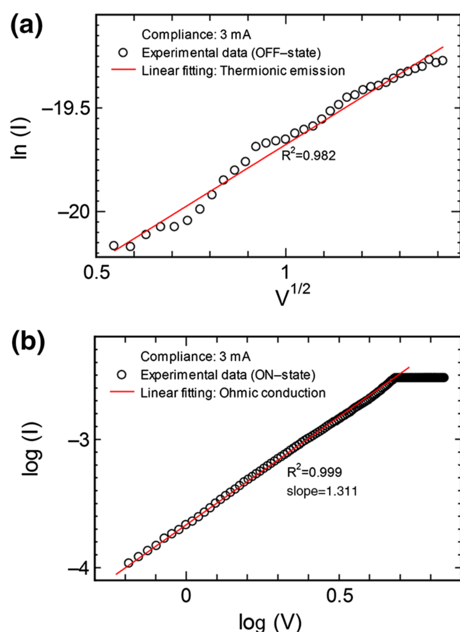

Fig. 4. Experimental and fitted I-V data for the ITO/PVP:TiO_2 NPs (8 wt.%)/Al memory device in the (a) OFF state and (b) ON state.

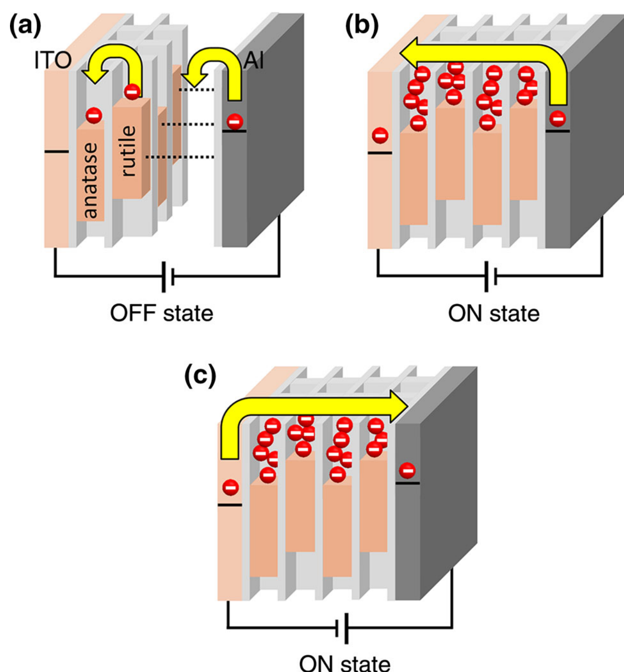

Fig. 5. Conduction mechanism of the ITO/PVP:TiO_2 NPs/Al bistable memory device: (a) the OFF state in the positive voltage, (b) the ON state in the positive voltage and (c) the ON state in the negative voltage.

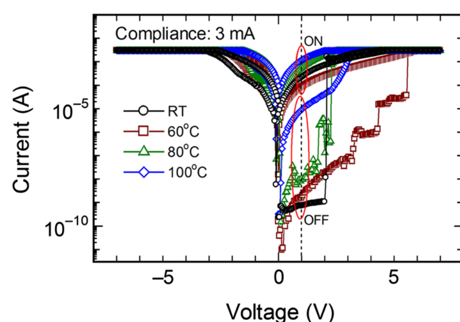

Fig. 6. Temperature dependency of I-V characteristics for the ITO/PVP:TiO_2 NPs (8 wt.%)/Al bistable memory device at different temperatures.

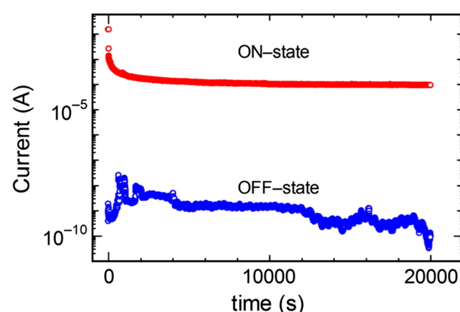

Fig. 7. Retention time measurement of the ITO/PVP:TiO_2 NPs (8 wt.%)/Al bistable memory device.

the electrons were blocked by the PVP blocking layer. At the same time, the electrons reversely injected from the ITO electrode and then transported to the Al electrode. As a result, the device could not return to the OFF state, as shown in Fig. 5c. However, some electrons leaked out from the trapping state and led to the device exhibiting minor hysteresis on the negative voltage (see Figs. 3 and 6).

It is well known that the thermionic emission and ohmic conduction show dependence on temperature. Therefore, the conduction mechanisms of the memory device were confirmed by a temperature dependence measurement with different selected cells. Figure 6 shows I-V temperature dependence characteristics for devices measured from room temperature (RT) to 100°C under a compliance current of 3 mA. For the ON and OFF states, results support thermionic emission and ohmic conduction mechanisms because relative temperatures of the I-V characteristics clearly influence current trends. The current of the ON and OFF states tends to increase with increasing temperature (read at +1 V, see Fig. 6).

The stored conductivities were tested using continuous readout in the ON and OFF states. Figure 7 shows the retention time characteristics of the ITO/PVP:TiO_2 NPs (8 wt.%)/Al bistable memory device. The OFF state was recorded at a constant reading voltage pulse of +1 V every 300 ms. The ON/OFF current ratios ($\sim 10^5$) were obtained after a voltage pulse of +7 V had been applied, and the ON state was recorded. However, the current in the OFF state shows a fluctuation current in a way that may be the result of instability in the trap states inside the layer. Nevertheless, the device exhibited two different current states for more than 20,000 s in each state.

Compared with other memory devices based on TiO_2 material, B. Mukherjee[34] found that TiO_2:-CuPc nanocomposite devices demonstrated the highest ON/OFF current ratio, $> 10^4$, with reading voltage at +0.5 V and rewritable memory. In addition, a single layer of PVK:TiO_2 composite film prepared by spin coating was reported by B. Cho[35] with the highest ON/OFF current ratio of about 10^5 at reading voltage +2 V. In our work, memory devices based on P-25 TiO_2 NPs composited with PVP film exhibited high ON/OFF current ratio, low reading voltage and also showed WORM memory.

CONCLUSION

In summary, the ITO/PVP:TiO_2 NPs/Al bistable memory device was successfully fabricated and investigated. The device showed two different states of current at a reading voltage of +1 V, with the highest ON/OFF current ratio of roughly 10^5. The optimal TiO_2 nanoparticle concentration at 8 wt.% was described with theoretical models. The electron transport mechanisms of the OFF and ON states were explained by thermionic emission and ohmic conduction, respectively. Moreover, the proposed conduction mechanisms of the bistable memory device were supported by temperature-dependent I-V measurements. In addition, retention time operations in the OFF and ON states were exhibited for more than 20,000 s in each state.

ACKNOWLEDGMENTS

This work was financially supported by King Mongkut's Institute of Technology Ladkrabang (KMITL, Grant No. A118-0260-079).

ELECTRONIC SUPPLEMENTARY MATERIAL

The online version of this article (https://doi.org/10.1007/s11664-019-07503-0) contains supplementary material, which is available to authorized users.

REFERENCES

1. P.H.C. Camargo, K.G. Satyanarayana, and F. Wypych, *Materials Research* 12, 1 (2009).
2. C.D. Tran, F. Prosenc, M. Franko, and G. Benzi, *A.C.S. Appl. Mater. Interfaces* 8, 34791 (2016).
3. Y. Qi, H. Qi, Y. He, W. Lin, P. Li, L. Qin, Y. Hu, L. Chen, Q. Liu, H. Sun, Q. Liu, G. Zhang, S. Cui, J. Hu, L. Yu, D. Zhang, and J. Ding, *ACS Appl. Mater. Interfaces* 10, 182 (2018).
4. R. Ambrosio, A. Carrillo, M. L. Mota, K. D. l. Torre, R. Torrealba, M. Moreno, H. Vazquez, J. Flores, and I. Vivaldo, *Polymers* 10, 1370 (2018).
5. L.D. Bozano, B.W. Kean, M. Beinhoff, K.R. Carter, P.M. Rice, and J.C. Scott, *Adv. Funct. Mater.* 15, 1933 (2005).
6. H. Wang, C. Zou, L. Zhou, C. Tian, and D. Fu, *Microelectron. Eng.* 91, 144 (2012).
7. K. Onlaor, T. Thiwawong, and B. Tunhoo, *J. Alloys Compd.* 732, 880 (2018).
8. M.A. Mamo, A.O. Sustaita, N.J. Coville, and I.A. Hümmelgen, *Org. Electron.* 14, 175 (2013).
9. S. Smith and S.R. Forrest, *Appl. Phys. Lett.* 84, 5019 (2004).
10. T.T. Dao, T.V. Tran, K. Higashimine, H. Okada, D. Mott, S. Maenosono, and H. Murata, *Appl. Phys. Lett.* 99, 233303 (2011).
11. J. Ouyang, *J. Mater. Chem. C* 3, 7243 (2015).
12. K. Onlaor, T. Thiwawong, and B. Tunhoo, *Org. Electron.* 31, 19 (2016).
13. S.M. Gupta and M. Tripathi, *Chinese Sci Bull* 56, 1639 (2011).
14. L. Qingjiang, A. Khiat, I. Salaoru, C. Papavassiliou, X. Hui, and T. Prodromakis, *Sci. Rep.* 4, 4522 (2014).
15. J. Ge and M. Chaker, *ACS Appl. Mater. Interfaces* 9, 16327 (2017).
16. M. Ravi, Y. Pavani, K. Kiran-Kumar, S. Bhavani, A.K. Sharma, and V.V.R. Narasimha-Rao, *Mater. Chem. Phys.* 130, 442 (2011).
17. V.V.R.N. Rao and A. Kalpalatha, *Polymer* 28, 648 (1987).
18. V.S. Reddy, S. Karak, S.K. Ray, and A. Dhar, *Org. Electron.* 10, 138 (2009).
19. P.T. Lee, T.Y. Chang, and S.Y. Chen, *Org. Electron.* 9, 916 (2008).
20. H.Y. Jeong, J.Y. Kim, T.H. Yoon, and S.Y. Choi, *Curr. Appl. Phys.* 10, e46 (2010).
21. J.H. Ham, D.H. Oh, S.H. Cho, J.H. Jung, T.W. Kim, E.D. Ryu, and S.W. Kim, *Appl. Phys. Lett.* 94, 112101 (2009).
22. W.S. Machado, M.A. Mamo, N.J. Coville, and I.A. Hümmelgen, *Thin Solid Films* 520, 4427 (2012).
23. S. Ali, J. Bae, C.H. Lee, K.H. Choi, and Y.H. Doh, *Org. Electron.* 25, 225 (2015).
24. D.H. Kim, W.K. Kim, S.J. Woo, C. Wu, and T.W. Kim, *Org. Electron.* 51, 156 (2017).
25. G. Liu, Q.D. Ling, E.Y.H. Teo, C.X. Zhu, D.S.H. Chan, K.G. Neoh, and E.T. Kang, *ACS Nano* 3, 1929 (2009).
26. T.T. Dao, T.V. Tran, K. Higashimine, H. Okada, D. Mott, S. Maenosono, and H. Murata, *Appl. Phys. Lett.* 99, 233303 (2011).
27. A. Rawat, H.K. Mahavar, S. Chauhan, A. Tanwar, and P.J. Singh, *Indian J. Pure Appl. Phys.* 50, 100 (2012).
28. P. Liu, Y. Wei, K. Jiang, Q. Sun, X. Zhang, S. Fan, S. Zhang, C. Ning, and J. Deng, *Phys. Rev. B* 73, 235412 (2006).
29. Q.D. Ling, D.J. Liaw, C. Zhu, D.S.H. Chan, E.T. Kang, and K.G. Neoh, *Prog. Polym. Sci.* 33, 917 (2008).
30. Z. Ji, Q. Mao, and W. Ke, *Solid State Commun.* 150, 1919 (2010).
31. F. C. Chiu, *Adv. Mater. Sci. Eng.* 2014, Article ID 578168 (2014).
32. T. Ohno, K. Sarukawa, K. Tokieda, and M. Matsumura, *J. Catal.* 203, 82 (2001).
33. V. Pfeifer, P. Erhart, S. Li, K. Rachut, J. Morasch, J. Brötz, P. Reckers, T. Mayer, S. Rühle, A. Zaban, I.M. Seró, J. Bisquert, W. Jaegermann, and A. Klein, *J. Phys. Chem. Lett.* 4, 4182 (2013).
34. B. Mukherjee, *J. Electron. Mater.* 48, 2131 (2019).
35. B. Cho, T.W. Kim, M. Choe, G. Wang, S. Song, and T. Lee, *Org. Electron.* 10, 473 (2009).

Publisher's Note Springer Nature remains neutral with regard to jurisdictional claims in published maps and institutional affiliations.